Articles

Energy Transfer Pathway in Luminescent Lanthanide Complexes Based on Dansyl-*N*-methylaminobenzoic Acid through Intramolecular Charge Transfer State for Near Infrared Emission

Soo-Gyun Roh, Nam Seob Baek, Yong Hee Kim,* and Hwan Kyu Kim†,*

*Department of Advanced Materials, Hannam University, Daejeon 306-791, Korea. *E-mail: josephin@mail.hannam.ac.kr*
*†Department of Chemistry, Korea University, Jochiwon, Chungnam 339-700, Korea. *E-mail: hkk777@korea.ac.kr*
Received May 10, 2007

We have investigated the photophysical properties of dansyl-*N*-methylaminobenzoic acid (DABAH) as a ligand and its lanthanide (Ln^{3+})-cored complexes (Ln^{3-}-$(DABA)_3$(terpy)) in order to determine the main energy transfer pathway for sensitized near infrared emission of Ln^{3-} ions (Ln^{3-} = Nd^{3+} and Er^{3+}) in Ln^{3+}-$(DABA)_3$(terpy). The fluorescence spectrum of DABAH shows a large Stokes shift with increasing solvent polarity. This large Stokes shift might be due to the formation of a twisted intramolecular charge transfer (TICT) state, as demonstrated by the large dipole moment in the excited state. It is in good agreement with the result that the phosphorescence even in the Gd^{3+}-cored complex based on the DABAH ligand was not observed, maybe due to the highly forbidden character of the $S_1 \rightarrow T_1$ transition in the DABAH ligand. A short decay component (*ca.* 1 ns) was observed in Er^{3+}-$(DABA)_3$(terpy) whereas the fluorescence lifetimes of DABAH and its Gd^{3-}-$(DABA)_3$(terpy) are observed about ~10 ns. The short component could be originated from the energy transfer process between the ligand and the Ln^{3-} ion. Based on the fluorescence of DABAH its Ln^{3+}-$(DABA)_3$(terpy), the sensitization of Ln^{3-} luminescence in the Ln^{3-}-$(DABA)_3$(terpy) takes place by the energy transfer *via* the TICT state of DABAH in the excited singlet state rather than *via* the excited triplet state.

Key Words : Luminescent lanthanide complexes, Dansyl-*N*-methylaminobenzoic acid, Energy transfer, Intramolecular charge transfer, Time-resolved luminescence

Introduction

Luminescent lanthanide complexes have been attracting considerable attention because of their academic interests and potential utility in a wide variety of photonic applications such as planar waveguide amplifiers, plastic lasers, light-emitting diodes, and luminescent probes.[1-5] The luminescent lanthanide complexes usually consist of Ln^{3-} ion and its chelating organic ligand as a photosensitizer. The emission of Ln^{3+} ion can be mainly observed by sensitization process upon the excitation of chelating organic moiety, since the organic chromophores have large molar absorption coefficient of several orders compared with those (typically 1-10 $M^{-1}cm^{-1}$) of Ln^{3+} ions.

The understanding of efficient energy transfer pathways is important in development of lanthanide complexes with a strong luminescent of Ln^{3+} ion. It is well-known that the sensitization of Ln^{3-} ion luminescence occurs through the excited triplet state of ligand, due to the heavy lanthanide ion effect.[6,7] Therefore, a lot of studies have been focused on developing the luminescent ligands in which the energy level of their triplet state of the luminescent ligands matches with the energy level of receiving Ln^{3-} ion to maintain efficient energy transfer from the triplet state to the lanthanide ion. However, a few articles reported that the energy transfer occurred from the excited singlet state to the Ln^{3-} ion.[8-10] Among them, van Veggel *et al.* reported that the energy transfer in dansyl- and lissamine-functionalized Nd^{3-} complexes occurred from the excited singlet state of the sensitizers to the Nd^{3+} ion. However, they did not consider the involvement of the intramolecular charge transfer (ICT) state in the excited state for the sensitized emission to Nd^{3-} ions, while dansyl derivatives tend to the easy formation of the ICT state in the excited state. For examples, Tong *et al.*[11] reported that the fluorescence of copolymerizable dansyl monomer shows the solvent polarity dependence. In this case, the emission maximum shifts from 463 nm in *n*-hexane to 530 nm in water. Fang *et al.*[12] also reported that the large Stokes shift was related to the ICT state in the excited state of a dansyl moiety immobilized on a chitosan film.

Generally, the ICT process in the organic molecules competes with the intersystem crossing (ISC) process. The ICT process of most organic chromophores is more dominant than the ISC process, because the rate of the ICT process is faster than the ISC process. Actually, Li *et al.*[13] reported no significant phosphorescence in 1-(dimethylamino)-5-naphthalenesulfonic amide (1,5-DNSA) with a noticeable ICT character, because this molecule shows the highly forbidden

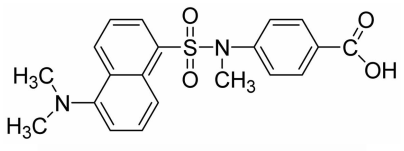

dansyl-N-methyl-aminobenzoic acid (DABAH)

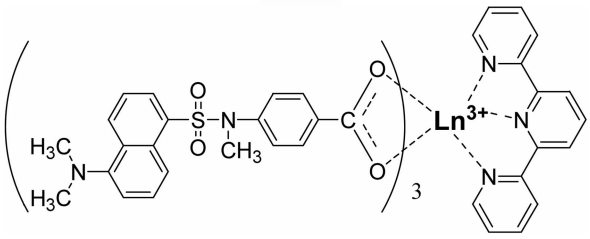

Ln^{3+}-$(DABA)_3$(terpy), Ln^{3+} = Gd^{3+}, Er^{3+}, Nd^{3+}

Scheme 1. Chemical structures of DABAH and Ln^{3+}-$(DABA)_3$-(terpy).

character of the $S_1 \rightarrow T_1$ transition.[14]

In this study, we have designed and synthesized dansyl-*N*-methylaminobenzoic acid (DABAH) as a sensitizer and its Ln^{3+}-$(DABA)_3$(terpy) in order to generate intense near infrared (near-IR) emission (Scheme 1).[15] We observed that the fluorescence emission of DABAH is markedly affected by solvent polarity. The Stokes shifted emission band of DABAH might be assigned as the TICT emission. This emission band was quenched in Ln^{3+}-$(DABA)_3$(terpy) and the near-IR emission of Ln^{3+} ion subsequently increased. We have found that the TICT state of the present ligand should play an important role in the energy transfer process between the ligand and Ln^{3+} ion in the excited state.

Experimental Section

The detail synthesis and characterization of DABAH and Ln^{3+}-$(DABA)_3$(terpy) were described in a previous report.[15] All solvents were the spectroscopic grade and used without further purification. The concentration of ligand and complexes was 2×10^{-5} M.

Absorption spectra were recorded on a Shimadzu UV-2401PC spectrophotometer. Luminescence and excitation spectra were measured by an Edinburgh FS920 fluorometer. Visible and near-IR luminescence spectra were detected with a PMT system (Hamamatsu R955) and a Ge-detector (Edinburgh Instruments EL-L) cooled with nitrogen, respectively. The quantum yields (ϕ_f) of ligand and complexes were determined using standard reference (Quinine sulfate in 0.05 N H_2SO_4, ϕ_f = 0.54).[14] The microsecond time-resolved emission measurements were carried out by using a Nd:YAG laser. The third harmonic generation (355 nm, 5 ns pulse width at 10 Hz repetition rate) of Nd:YAG laser (EXSPLA NT342) system was used to excite the ligand moiety. The emission spectrum was analyzed with a monochromator (Acton spectrapro 2300i) and detected with a photomultiplier followed by a boxcar averager (Stanford Research System) or a digital oscilloscope (Agilent infinium 54832B DSO). Temporal profiles of the photoluminescence (PL) decays on ns ~ ps time scale were measured by using time-correlated single photon counting method (TCSPC). The excitation source is a self-mode locked picosecond Ti-Sapphire laser (Coherent Model Mira TM 900) pumped by an Nd:YVO_4 laser (Coherent Verdi TM diode-pumped laser). The laser output has ~3 ps pulse width, and it can span the excitation wavelength in the range of 350-490 nm by second-harmonic generation. All the standard electronics for the TCSPC were from the Edinburgh Instruments. The instrument response function was measured by detecting the scattered laser pulse of 3 ps with quartz crystal. The resultant FWHM is 70 ps. The best fit of the decay was determined by monitoring the value of χ^2 and the values are about 0.99. Geometry Optimization was carried out using the DFT method for the ground-state with B3LYP/6-31G(d) basis set employing the Gaussian 98 program package.

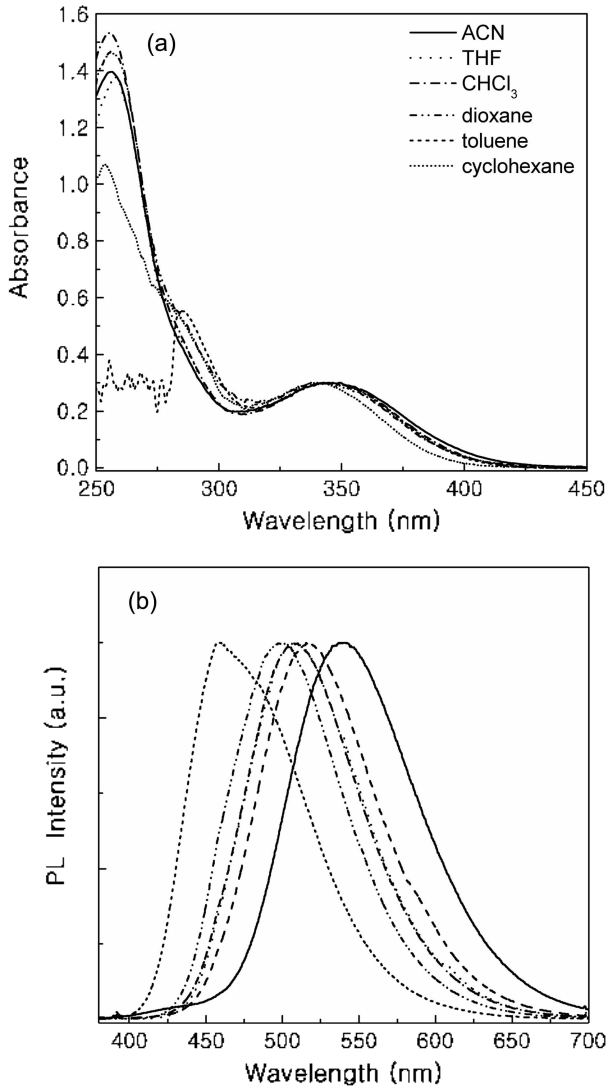

Figure 1. Absorption (a) and emission (b) spectra of DABAH in various solvents (concentration 2.0×10^{-5} M) with an excitation at 350 nm.

Results

Absorption and Fluorescence Spectral Properties of DABAH

Steady-State Spectral Properties. The absorption and fluorescence spectra of free ligand (DABAH) in various solvents are shown in Figure 1(a). Two absorption bands around 260 and 350 nm were observed. The molar extinction coefficient of 260 nm (ε_t = 15000-18000) is larger than that of the 350 nm (ε_t = 3000), indicating that the former one may be attributed to the pure π, π^* transition. The latter one was slightly red-shifted as the solvent polarity increases. It implies that the absorption band of 340 nm is also attributed to the π, π^* transition. The small change of the absorption bands implies that the electronic nature in the ground state is not changed in different solvents.

In contrast to a weak solvent-dependence on the absorption spectra, the DABAH ligand also shows an outstanding solvatochromic emission behavior. It is known that the solvent polarity effect was analyzed in terms of difference in the dipole moments in the ground and excited states, and it has been found that the larger dipole-moment change causes larger emission band shift. The dipole moment change between the ground state and the excited state is calculated from the slope of the Lippert-Mataga plot given in eq. (1),[16] which is essentially a plot of the Stokes shift of the emission versus the solvent polarity.

$$\bar{\upsilon}_a - \bar{\upsilon}_f = \frac{2}{hc} \times \left(\frac{\varepsilon - 1}{2\varepsilon + 1} - \frac{n^2 - 1}{2n^2 + 1} \right) \times \frac{(\mu_e - \mu_g)^2}{a^3} \qquad (1)$$

Where, $\bar{\upsilon}_a - \bar{\upsilon}_f$ is the Stokes shift, μ_e and μ_g are the dipole moments of the excited and ground state, respectively, h is Planck constant, c is the speed of light in vacuum and 'a' is the radius of Onsager cavity around the fluorophore. The Stokes shift of DABAH fluorescence as a function of solvent polarity parameter is shown in Figure 2, according to eq. (1). The Onsager radius, 'a', of DABAH is calculated to be 11.4 Å. From the slope of the straight line, the difference between the dipole moment of excited state and ground state ($\mu_e - \mu_g$) is evaluated to be 30.1 Debye.

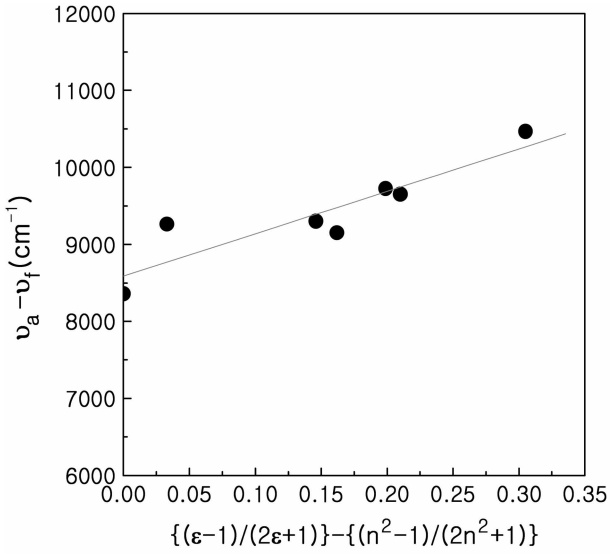

Figure 2. The Stokes' shift of DABAH fluorescence as a function of solvent polarity parameters. The number refer to the following solvents: 1: ACN, 2: THF, 3: EA, 4: ethyl ether, 5: chloroform, 6: dioxane, 7: cyclohexane.

Table 1. Fluorescence quantum yield and decay time constants (ns) of DABAH in various solvents

Solvents	$\lambda^{fl}_{max.}$	ϕ_f	Fluorescence decay time, ns	
			460 nm	560 nm
ACN	540	0.16	1.5 (0.16)	
			9 (0.84)	9 (1)
Chloroform	510	0.46	13 (1)	13 (1)
Dioxane	507	0.55	16 (1)	16 (1)
toluene	498	0.45	11 (1)	11 (1)
Cyclohexane	455	0.49	10 (1)	10 (1)

Time-resolved Emission Properties. In order to understand the excited state dynamics of DABAH, we have measured the time-resolved fluorescence decays in various solvents with an excitation at 370 nm. The fluorescence decay profiles were measured at 460 nm and 560 nm, which individually corresponds to the emission maximum wavelength in nonpolar solvent (cyclohexane) and polar solvent (ACN), respectively. The fluorescence decay times of DABAH in various solvents are summarized in Table 1.

The emission decay profile of DABAH, monitored at 560 nm, shows the decay time constants of 8-16 ns which was fitted using a single exponential function. The fluorescence emission decay profile, monitored at 460 nm, also exhibits the mono exponential decay, except for ACN. In highly polar solvent, ACN, the fluorescence decay profiles, probed at 460 nm, shows the bi-exponential decay including an additionally new faster decay time of 1.5-2 ns.

Fluorescence Spectral Properties of Ln^{3+}-$(DABA)_3$-(terpy)

Fluorescence of Ligand in Ln^{3+}-$(DABA)_3$(terpy). We attempted to measure the fluorescence spectra of Ln^{3+}-$(DABA)_3$(terpy) in ACN and chloroform, because the solubility is very low in other organic solvents. Figure 3 shows the fluorescence spectra of DABAH and Nd^{3+}-$(DABA)_3$(terpy) and Gd^{3+}-$(DABA)_3$(terpy) in ACN and chloroform. Upon the photoexcitation at the absorption maximum wavelength of the corresponding ligand in Nd^{3+}-$(DABA)_3$(terpy), the emission intensity of the ligand in Nd^{3+}-$(DABA)_3$(terpy) is significantly diminished, as compared with that of the free DABAH. The results were listed in Table 2. The quantum yield of the fluorescence of DABAH is 15% for Gd^{3+}-$(DABA)_3$(terpy), 3% for Nd^{3+}-$(DABA)_3$(terpy) and 6% for Er^{3+}-$(DABA)_3$(terpy) in ACN. Assuming that the paramagnetic effects of Nd(III) and Er(III) are almost equal to that of Gd(III), the energy transfer efficiency is calculated using the ratio of DABAH intensity in the Gd^{3+}-$(DABA)_3$(terpy), Nd^{3+}-$(DABA)_3$(terpy) and Er^{3+}-$(DABA)_3$(terpy)energy. The energy transfer efficiency

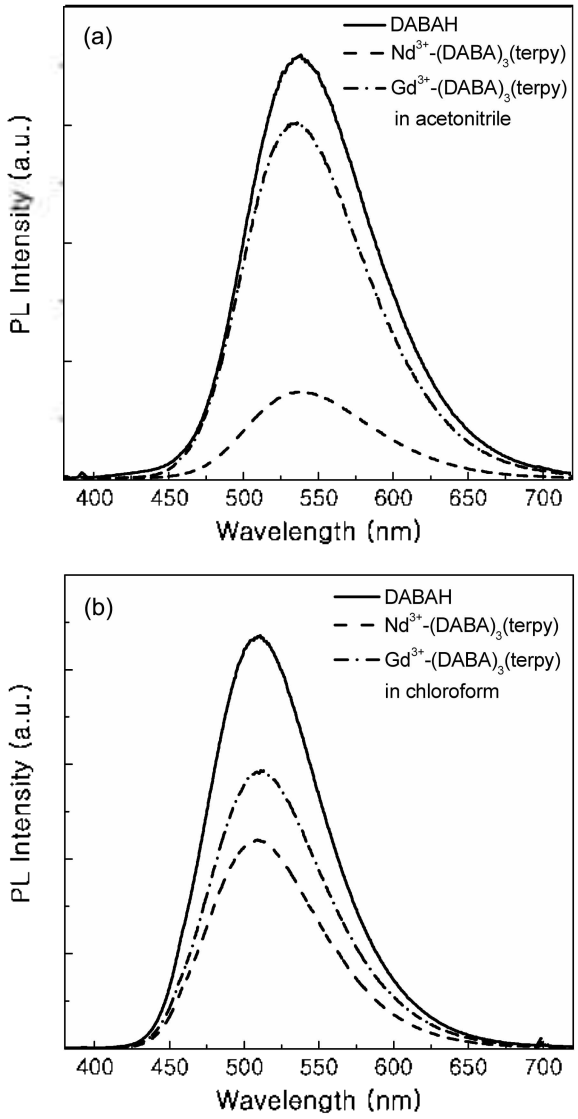

Figure 3. Emission spectra of DABAH and Ln^{3+}-$(DABA)_3$(terpy) (concentration 2×10^{-5} M) with an excitation at 350 nm.

(ϕ_{ET}) were 0.8 and 0.6 for Nd^{3+}-$(DABA)_3$(terpy) and Er^{3+}-$(DABA)_3$(terpy) in ACN, respectively. In chloroform, the energy transfer efficiency were 0.26 and 0.52 for Nd^{3+}-$(DABA)_3$(terpy) and Er^{3+}-$(DABA)_3$(terpy).

Time-resolved Emission Spectral Properties of Ln^{3+}-$(DABA)_3$(terpy). The fluorescence lifetimes of DABAH in Ln^{3+}-$(DABA)_3$(terpy) were monitored at 550 nm and summarized in Table 2. The fluorescence decay profiles of the ligand in Nd^{3+}-$(DABA)_3$(terpy) show a bi-exponential decay with luminescence lifetimes of 0.5 (56%) and 9 ns (44%) in ACN, and 0.6 (26%) and 13 ns (74%) in chloroform, respectively. The fast decay component in Nd^{3+}-$(DABA)_3$(terpy) is considered to be the energy transfer efficiency, and the slow decay component has the same as the decay time of the DABAH ligand. The amplitude of the fast decay component is larger in ACN (56%) than in chloroform (26%). It means that the energy transfer efficiency of Nd^{3+}-$(DABA)_3$(terpy) is higher in ACN than in chloroform. Whereas the fluorescence decay profiles of the ligand in the Gd^{3+}-$(DABA)_3$(terpy) show a mono-exponential decay with the lifetimes of *ca.* 9 ns in ACN and 12-13 ns in chloroform, respectively.

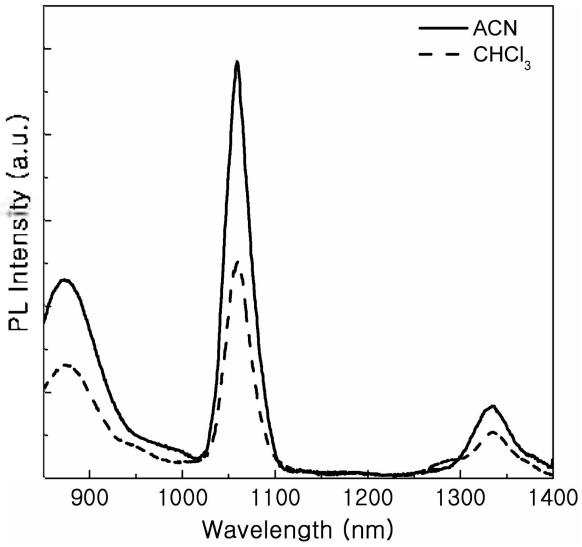

Figure 4. Emission spectra of sensitized Nd^{3+} ion in Nd^{3+}-$(DABA)_3$(terpy) with an excitation at 350 nm.

Sensitized near-IR Luminescence, Lifetime and Quantum Yield of Ln^{3+} Ions. Figure 4 shows the sensitized near-IR Nd^{3+} emission in Nd^{3+}-$(DABA)_3$(terpy) in ACN and chloroform. Upon the photoexcitation at the absorption maximum wavelength of the corresponding ligand at 350 nm, the typical emission lines are observed at 890 nm ($^4F_{3/2} \rightarrow {}^4I_{9/2}$), 1064 nm ($^4F_{3/2} \rightarrow {}^4I_{11/2}$) and 1330 nm ($^4F_{3/2} \rightarrow {}^4I_{13/2}$) for Nd^{3+} ion, and at 1525 nm ($^4I_{13/2} \rightarrow {}^4I_{15/2}$) for Er^{3+} ion. The

Table 2. Photophysical parameters for DABAH and Ln^{3+}-$(DABA)_3$(terpy)

	ACN					Chloroform				
	ϕ_f	τ^a (ns)	$\tau_{obs}{}^b$ (ns)	k_{ET} (s^{-1})	ϕ_{Ln}	ϕ_f	τ^a (ns)	$\tau_{obs}{}^b$ (ns)	k_{ET} (s^{-1})	ϕ_{Ln}
DABAH	0.16	9 (1)[c]	–	–	–	0.46	13 (1)	–	–	–
Gd^{3+}-$(DABA)_3$(terpy)	0.15	9.5 (1)[c]	–	–	–	0.31	12 (1)	–	–	–
Nd^{3+}-$(DABA)_3$(terpy)	0.03	0.5 (0.56)[c] 9 (0.44)[c]	130	1.9×10^9	5.2×10^{-4}	0.23	0.6 (0.26) 13 (0.74)	70	1.6×10^9	2.8×10^{-4}
Er^{3+}-$(DABA)_3$(terpy)	0.06	1.5 (0.54)[c] 9 (0.46)	110	5.6×10^8	1.6×10^{-5}	0.1	1 (0.32) 13 (0.68)	60	9.2×10^8	7.5×10^{-6}

[a]decay times for DABAH in Ln^{3+}-$(DABA)_3$(terpy). [b]decay times for Ln^{3+} ions in near IR emission.

sensitized emission intensity of both Nd^{3+} and Er^{3+} ion in Ln^{3-}-$(DABA)_3$(terpy) is stronger in ACN than in chloroform.

Furthermore, the lifetimes of the sensitized Ln^{3+} ion were measured by using time-resolved emission spectroscopy with the excitation wavelength at 355 nm in ACN and chloroform. The time-resolved luminescence spectra in the near IR region show monoexponential decays. The fluorescence decays of Ln^{3-}-$(DABA)_3$(terpy) were monitored at 1060 nm for Nd^{3-}-$(DABA)_3$(terpy) and at 1525 nm for Er^{3+}-$(DABA)_3$(terpy), respectively. In ACN, the decay times of both Nd^{3-} and Er^{3+} ion in Ln^{3-}-$(DABA)_3$(terpy) are 130 and 110 ns, respectively. The decay times of both Nd^{3+} and Er^{3+} ion in chloroform are 70 and 60 ns, respectively (see Table 2). For Nd^{3-}-$(DABA)_3$(terpy) and Er^{3-}-$(DABA)_3$(terpy), the luminescence quantum yields ($\phi_{Ln} = \tau_{obs}/\tau_R$) of Ln^{3+} ions were determined from the observed lifetimes ($\tau_{obs} = (k_r + k_{nr})^{-1}$) and the radiative lifetimes ($\tau_R = k_r^{-1}$) of the Ln^{3+} ions. The radiative lifetimes were taken from the literature.[17] with the typical lifetimes of 8 ms for Er^{3-} ion and 0.25 ms for Nd^{3+} ion, respectively. Calculated intrinsic quantum yields of near IR emission for Nd^{3-} and Er^{3-} ions were summarized in Table 2.

Discussion

Twisted Intramolecular Charge Transfer State of DABAH. Our solvent dependence study for the fluorescence of DABAH shows a possibility of the large dipole moment change in the excited state. The ICT process in the DABAH may easily take place even in nonpolar solvent. It may be due to its structural feature as follows: The DABAH ligand has non-planar structure in the ground state, in which the naphthalene group is placed out-of-plane with respect to the amino group bridged by sulfone (Scheme 1). Therefore, its chemically structural feature could allow the ICT state of DABAH to be formed easily in the excited state without regarding to the solvent polarity. Actually, the emission maximum (450 nm) of DABAH is already shifted to be ~6500 cm^{-1} and it may be originated from the ICT state. It was noteworthy that the fluorescence spectrum of DABAH in cyclohexane shows a nonsymmetrical spectral shape, fitted with two Gaussian functions which are resolved into two emission bands having the wavelength maxima at 450 nm and 490 nm. These results suggest emission from at least two different emitting states which may be due to the intramolecular charge transfer (ICT) state and the twisted intramolecular charge transfer (TICT) states. The fluorescence of DABAH in polar solvent (ACN) shows only the large Stokes shifted emission which is due to the TICT state of DABAH and we could not observe the normal emission of nonplanar DABAH.

Usually, the TICT molecules show the dual emission bands[18,19] which are originated from the normal excited state and the TICT state. Interestingly, the fluorescence spectra of *p*-aminobenzophenone (*p*-ABP)[20] were shifted to the longer wavelength as the solvent polarity increases. The large Stokes shifted fluorescence emission of *p*-ABP in polar solvents was considered to be the formation of the TICT state, which is stabilized by solvating with polar solvents. However, *p*-ABP shows only one broad emission at the long wavelength. In other words, *p*-ABP did not show the dual emission, although the *p*-ABP is known as the TICT molecules. And also, ultrafast relaxation dynamics studies on the emission of Michler's ketone indicated that the maximum of fluorescence band depends on solvent polarity and a large Stokes shifted emission is originated from the TICT state.

The fluorescence decay of DABAH is also not resolved into the bi-exponential decay in nonpolar and moderately polar solvents although the emission bands of DABAH in cyclohexane are originated from the ICT and TICT state. It may be due to the fact that the ICT emission at 460 nm is strongly overlapped with the TICT emission band. On the other hand, in highly polar solvent, ACN, the fluorescence decay profiles, probed at 460 nm, show the bi-exponential decay including an additionally faster decay time of 1.5-2 ns . In the polar solvent, such as ACN, the TICT emission is more stabilized than in other solvents. As a result, we could distinguish the ICT emission with the fast decay time of 1.5 ns (16%) from the TICT emitting species with the slow decay time of 9 ns (84%).

Sensitized Emission of Ln^{3+} Ions in Ln^{3+}-$(DABA)_3$-(terpy). Gd^{3-} ion has no energy levels of below 32,000 cm^{-1} and the fluorescence emission of DABAH was observed in the region of 22,200-15,500 cm^{-1}. From this result, the energy levels of Gd^{3-} ion do not match with any excited singlet and/or triplet state of DABAH. If Gd^{3-}-$(DABA)_3$-(terpy) has the high ISC efficiency by the heavy metal effect, the significant fluorescence intensity reduction of the ligand in Gd^{3+}-$(DABA)_3$(terpy) might be expected by the formation of the lowest triplet state of the DABAH ligand in the complex. However, there is no significant reduction of emission intensity for the present ligand in Gd^{3-}-$(DABA)_3$-(terpy). It implies that the Gd^{3+} ion in the present complex cannot provide an external heavy atom effect, and the Gd^{3-} ion does not lead to the ISC process. It is confirmed by no significant phosphorescence detection for Gd^{3-}-$(DABA)_3$-(terpy) even at 77 K. Therefore, we could exclude the role of excited triplet state on the possible energy transfer pathways between the Ln^{3+} ion and the ligand. Based on these results, we can suggest that the reduction of the fluorescence quantum yield of ligand in Ln^{3-}-$(DABA)_3$(terpy) could be due to the energy transfer from the TICT state of DABAH to the Ln^{3+} ion.

We have also investigated the fluorescence behaviors for the free ligand and Nd^{3+}-$(DABA)_3$(terpy) in chloroform, as a less polar solvent. The ligand fluorescence intensity in Nd^{3-}-$(DABA)_3$(terpy) was also reduced, as compared with that of the free corresponding ligand. It indicates that even in a less polar solvent of chloroform, the energy transfer takes place in Nd^{3-}-$(DABA)_3$(terpy) effectively. The reduced fluorescence intensity in Gd complex may be due to induced intersystem crossing or to a perturbation change on the fluorescent ligand. In the first case, the triplet state of dansyl

unit should be formed and the phosphorescence of T_1 in rigid matrix should be observed. However, PL spectrum shows no evidence of phosphorescence although the ligand fluorescence in chloroform is more quenched than in ACN. We are therefore inclined to attribute the quenching effect to a perturbation on the excited state.

The estimated quantum yield of the energy transfer (ϕ_{LT}) was 0.8 in ACN and 0.26 in chloroform for Nd^{3-}-$(DABA)_3$(terpy) (Table 2). This could imply that the energy transfer occurs more effectively in ACN than in chloroform. As discussed previously, the spectral dependency studies of the DABAH ligand on solvent polarity strongly support the presence of its TICT state in moderately polar solvent as well as highly polar solvents, according to the large dipole moment value in the excited state. Thus, we can suggest that the TICT state might be involved in the energy transfer pathway for the Ln^{3-}-$(DABA)_3$(terpy).

The decay profiles of the ligand in Ln^{3+}-$(DABA)_3$(terpy) show a bi-exponential of a fast component and a relatively slow component. We might ascribe to the presence of two distinct populations of the present complexes: one long-lived component, which is responsible for no energy transfer and has a same decay time as observed in Gd^{3+}-$(DABA)_3$(terpy), and the other fast component which is responsible for the energy transfer through the TICT state to the Ln^{3+} ion. And also, the fast decay time of 1.5 ns in Er^{3-}-$(DABA)_3$(terpy) is 3 times longer than that of 0.5 ns in Nd^{3+}-$(DABA)_3$(terpy) in ACN. It implies that the energy transfer rate between the ligand and Er^{3+} ion in Er^{3+}-$(DABA)_3$(terpy) is slower than the rate between the ligand and Nd^{3+} ion in Nd^{3-}-$(DABA)_3$-(terpy).

The intrinsic quantum yield for Nd^{3-} ion emission is comparable with the other report. However, the significantly lower quantum yield was observed for Er^{3-} ion. The sensitized luminescence consists of i) the excitation of the DABAH into its TICT state, ii) the energy transfer from the TICT state to the resonance level of Ln^{3-} ion, and the subsequent relaxation to the emission level. Considering this pathway, the overall quantum yield of the sensitized luminescence can be expressed as

$$\frac{\tau}{\tau_0} = \Phi_{antenna}\Phi_{ET}\Phi_{rel} \qquad (2)$$

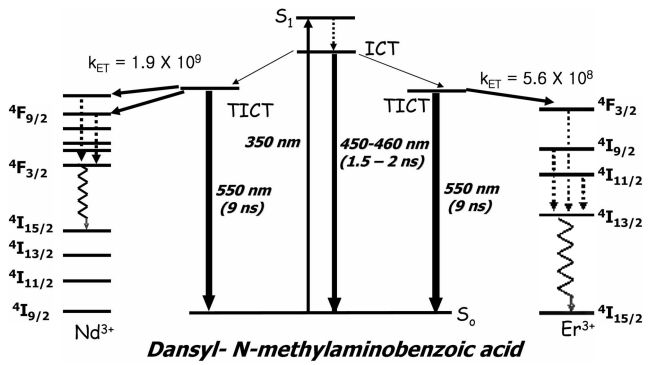

Scheme 2. Schematic diagram of the photophysical processes leading to sensitized Ln^{3+} luminescence of Ln^{3-}-$(DABA)_3$(terpy).

Where the quantum yield of the Gd(III) complex is taken $\Phi_{antenna}$ and Φ_{rel} is the relaxation efficiency strongly associated with raditionless transition. Substituting the experimentally determined values of $\Phi_{antenna}$ and Φ_{ET} into equation (2), we obtained Φ_{rel} = 0.4% for Nd^{3-}-$(DABA)_3$(terpy) and 0.02% for Er^{3-}-$(DABA)_3$(terpy). The energy loss during the relaxation for Er^{3+}-$(DABA)_3$(terpy) was much greater than that for Nd^{3+}-$(DABA)_3$(terpy). This may be due to the larger energy gap (ΔE) between the TICT state of DABAH and the efficient quenching of the long lived excited state of Er^{3+} ion with C-H vibration overtones.

Conclusions

We have prepared DABAH and its Ln^{3-}-$(DABA)_3$(terpy) in order to establish the main energy transfer pathway for sensitized near-IR emission of Ln^{3+} ions, such as Gd^{3+}, Nd^{3-}, and Er^{3+} ions. In contrast to other Ln^{3+} complexes in which the energy transfer includes the excited triplet state, the sensitization of Ln^{3-} ion luminescence in Ln^{3+}-$(DABA)_3$-(terpy) takes place from the excited singlet state of DABAH. The large Stokes shift of the DABAH emission with increasing solvent polarity supports the formation of the TICT state in the excited singlet state. Also, the energy transfer efficiency and the quantum efficiency of sensitized emission of Er^{3-} and Nd^{3-} ions exhibit the good dependency on the solvent polarity. Therefore, the TICT state can be suggested as a main pathway for the generation of sensitized Ln^{3-} luminescence in Ln^{3-}-$(DABA)_3$(terpy).

Acknowledgment. This study was supported by the Korea Research Foundation Grant (R03-2004-000-10017-0).

References

1. (a) Kim, H. K.; Roh, S.-G.; Hong, K.-S.; Ka, J.-W.; Back, N. S.; Oh, J. B.; Nah, M. K.; Cha, Y. H.; Ko, J. *Macromol. Res.* **2003**, *11*, 133. (b) Kim, H. K.; Oh, J. B.; Back, N. S.; Roh, S.-G.; Nah, M. K.; Kim, Y. H. *Bull. Korean Chem. Soc.* **2005**, *26*, 201. (c) Baek, N. S.; Kim, Y. H.; Roh, S.-G; Kwak, B. K.; Kim, H. K. *Adv. Funct. Mater.* **2006**, *16*, 1873. (d) Kim, Y. H.; Baek, N. S.; Oh, J. B.; Nah, M. K.; Roh, S. G; Song, B. J.; Kim, H. K. *Macromol. Res.* **2007**, *15*, 272.
2. Shavaleev, N. M.; Moorcraft, L. P.; Pope, S. J. A.; Bell, Z. R.; Faulkner, S.; Ward, M. D. *Chem. Eur. J.* **2003**, *9*, 5283.
3. Kawa, M.; Frechet, J. M. J. *Chem. Mater.* **1998**, *10*, 286.
4. Destri, S.; Porzio, W.; Meinardi, F.; Tubino, R.; Salerno, G. *Macromol.* **2003**, *36*, 273.
5. Kang, T.-S.; Harrison, B. S.; Foley, T. J.; Knefely, A. S.; Boncella, J. M.; Reynolds, J. R.; Schanze, K. S. *Adv. Mater.* **2003**, *15*, 1093.
6. (a) Reinhoudt, D. N.; van Veggel, F. C. J. M.; Werts, M. H. V.; Geurts, F. A. J. J.; Hofstraat, W. *J. Phys. Chem. A* **2000**, *104*, 5457. (b) Slooff, L. H.; Polman, A.; Cacialli, F.; Friend, R. H.; Hebbink, G. A.; van Veggel, F. C. J. M.; Reinhoudt, D. N. *Appl. Phys. Lett.* **2001**, *78*, 2122.
7. (a) Oh, J. B.; Nah, M.-K.; Kim, Y. H.; Kim, H. K. *J. Luminescence* **2005**, *111*, 255. (b) Oh, J. B.; Nah, M.-K.; Kim, Y. H.; Kang, M. S.; Ka, J.-W.; Kim, H. K. *Adv. Funct. Mater.* **2007**, *17*, 413.
8. Yang, C.; Fu, L.-M.; Wang, Y.; Zhang, J.-P.; Ai, W.-T.; Wong, X.-C.; Qiao, Y.-F.; Zuo, B.-S.; Gui, L.-L. *Angew. Chem. Int. Ed.*

2004. *43*, 5010.
9. Hebbink, G. A.; Klink, S. I.; Grave, L.; Alink, P. G. B. O.; van Veggel, F. C. J. M. *ChemPhysChem* **2002**, *3*, 1014.
10. Vicinelli, V.; Ceroni, P.; Maestri, M.; Balzani, V.; Gorka, M.; Vogtle, F. *J. Am. Chem. Soc.* **2002**, *124*, 6461.
11. Ren, H.; Gao, F.; Tong, Z.; Yan, Y. *Chem. Phys. Lett.* **1999**, *307*, 55.
12. Ding, L.; Fang, Y.; Jiang, L.; Gao, L.; Yin, X. *Thin Solid Films* **2005**, *478*, 318.
13. Li, Y.-H.; Chan, L.-M.; Tyer, L.; Moody, R. T.; Himel, C. M.; Hercules, D. M. *J. Am. Chem. Soc.* **1975**, *97*, 3118.
14. (a) Kim, Y. H.; Baek, N. S.; Kim, H. K. *ChemPhysChem* **2006**, *7*, 213. (b) Kim, Y. H.; Baek, N. S.; Kim, H. K. *Bull. Korean Chem. Soc.* **2006**, *27*, 1729.
15. Roh, S.-G.; Kim, Y. H.; Baek, N. S.; Hong, K.-S.; Kim, H. K. *Mol. Cryst. & Liq. Cryst.* **2006**, *446*, 295.
16. Mataga, N.; Kaifu, Y.; Koizumi, M. *Bull. Chem. Soc. Jpn.* **1956**, *29*, 465.
17. (a) Magennis, S. W.; Ferguson, A. J.; Bryden, T.; Jones, T. S.; Beeby, A.; Samual, I. D. W. *Synthetic Metal* **2003**, *138*, 463. (b) Weber, M. *J. Phys. Rev.* **1968**, *171*, 283.
18. Druzhinin, S. I.; Demeter, A.; Zachariasse, K. A. *Chem. Phys. Lett.* **2001**, *347*, 421.
19. Glasbeek, M.; Zhang, H. *Chem. Rev.* **2004**, *104*, 1929.
20. Singh, A. K.; Bhasikuttan, A. C.; Palit, D. K.; Mittal, J. P. *J. Phys. Chem. A* **2000**, *103*, 7002.
21. Mondal, J. A.; Ghosh, H. N.; Ghanty, T. K.; Mukherjee, T.; Palit, D. K. *J. Phys. Chem. A* **2006**, *110*, 3432.